

Design of a homologous series of molecular glassformers

Cite as: J. Chem. Phys. **155**, 224503 (2021); <https://doi.org/10.1063/5.0066410>

Submitted: 10 August 2021 • Accepted: 16 November 2021 • Published Online: 10 December 2021

 Sarah E. Wolf, Tianyi Liu,  Shivajee Govind, et al.

COLLECTIONS

Paper published as part of the special topic on [Slow Dynamics](#)



View Online



Export Citation



CrossMark

ARTICLES YOU MAY BE INTERESTED IN

[Gradient in refractive index#reveals denser near free surface region in thin polymer films](#)

The Journal of Chemical Physics **155**, 144901 (2021); <https://doi.org/10.1063/5.0062054>

[The relaxation behavior of supercooled and glassy imidacloprid](#)

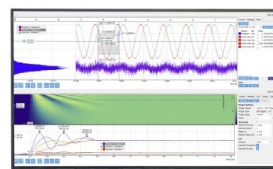
The Journal of Chemical Physics **155**, 174502 (2021); <https://doi.org/10.1063/5.0067404>

[Interconversion-controlled liquid-liquid phase separation in a molecular chiral model](#)

The Journal of Chemical Physics **155**, 204502 (2021); <https://doi.org/10.1063/5.0071988>

Challenge us.

What are your needs for
periodic signal detection?



Zurich
Instruments

Design of a homologous series of molecular glassformers

Cite as: J. Chem. Phys. 155, 224503 (2021); doi: 10.1063/5.0066410

Submitted: 10 August 2021 • Accepted: 16 November 2021 •

Published Online: 10 December 2021



View Online



Export Citation



CrossMark

Sarah E. Wolf, Tianyi Liu, Shivajee Govind, Haoqiang Zhao, Georgia Huang, Aixi Zhang, Yu Wu, Jocelyn Chin, Kevin Cheng, Elmira Salami-Ranjbaran, Feng Gao, Gui Gao, Yi Jin, Youge Pu, Thiago Gomes Toledo, Keyume Ablajan, Patrick J. Walsh, and Zahra Fakhraei

AFFILIATIONS

Department of Chemistry, University of Pennsylvania, Philadelphia, Pennsylvania 19104, USA

Note: This paper is part of the JCP Special Topic on Slow Dynamics.

^{a)}Authors to whom correspondence should be addressed: pwalsh@sas.upenn.edu and fakhraei@sas.upenn.edu

ABSTRACT

We design and synthesize a set of homologous organic molecules by taking advantage of facile and tailorable Suzuki cross coupling reactions to produce triarylbenzene derivatives. By adjusting the number and the arrangement of conjugated rings, the identity of heteroatoms, lengths of fluorinated alkyl chains, and other interaction parameters, we create a library of glassformers with a wide range of properties. Measurements of the glass transition temperature (T_g) show a power-law relationship between T_g and molecular weight (M_w), with of the molecules, with an exponent of 0.3 ± 0.1 , for T_g values spanning a range of 300–450 K. The trends in indices of refraction and expansion coefficients indicate a general increase in the glass density with M_w , consistent with the trends observed in T_g variations. A notable exception to these trends was observed with the addition of alkyl and fluorinated alkyl groups, which significantly reduced T_g and increased the dynamical fragility (which is otherwise insensitive to M_w). This is an indication of reduced density and increased packing frustrations in these systems, which is also corroborated by the observations of the decreasing index of refraction with increasing length of these groups. These data were used to launch a new database for glassforming materials, glass.apps.sas.upenn.edu.

Published under an exclusive license by AIP Publishing. <https://doi.org/10.1063/5.0066410>

I. INTRODUCTION

The dynamics of a supercooled liquid (SCL) drastically slows upon cooling toward the glass transition temperature (T_g) such that for every few degrees of cooling, the structural relaxation time (τ_α) and viscosity (η) increase by a decade.^{1–3} As such, the glass transition temperature, T_g , depends on the cooling rate. T_g is conventionally defined at a cooling rate of $CR \sim 10$ K/min, corresponding to $\tau_\alpha \sim 100$ s for most systems.^{3,4} In molecular glasses and polymers within a homologous series, T_g has been shown to generally increase with the molecular weight (M_w)^{5–12} through a power-law relationship, $T_g \propto M_w^\nu$, where $0.3 < \nu < 0.5$.^{10,12,13} These observations are consistent with theoretical predictions of the molecular weight dependence of T_g .^{14–17} However, strong intermolecular interactions^{13,18} and variations of intra-molecular degrees of freedom can affect the value of T_g and a molecule's glass-forming ability.^{19,20} Systematic studies of the effect of interactions, structural motifs, and network formation on glass transition have

been explored in systems such as metallic alloys,²¹ network forming glasses,^{22–26} and ionic liquids.^{27–29} Molecular dynamics simulations have also shown T_g to be related to packing details and density.³⁰

The dynamic fragility index (m) is also an important factor in characterizing thermal properties of supercooled liquids close to their T_g . m , normalized activation energy at T_g , is a measure of the degree of non-Arrhenius behavior of a glassy system. Most molecular glasses^{31–35} and polymers³⁶ display a fragile behavior with large values of m . In contrast to T_g , fragility is typically not a strong function of M_w and is instead affected by factors such as mechanical properties,³⁷ side-chain flexibility in polymers,³⁸ or shape anisotropy in molecular glasses.³⁰ However, some studies suggest that a weak linear correlation may still exist between fragility and T_g .³⁹ It has also been suggested that m is an increasing function of the product of T_g and the glass expansion coefficient (α).^{40,41} As such, for systems with similar expansion coefficients, an apparent dependence of m on T_g and therefore M_w may still be observed. The dependence

of fragility on α and the molecular level interactions highlights the important role of the local interaction potential and its anharmonicity⁴² on the properties of supercooled liquids.

Given this complexity of their behavior, understanding the structure/property relationships in molecular glassformers is critical in designing new materials for specific applications. Predictive models and algorithms have indeed been used to estimate T_g and fragility in molecular glasses^{43–46} and polymers.⁴⁷ Structure/property relationships have also become more critical in studies of stable vapor-deposited glasses.⁴⁸ In these systems, in addition to the deposition conditions, T_g and fragility,⁴⁹ the thermal stability and glass structure also depend on factors such as hydrogen bonding and other intermolecular interactions^{50–54} and molecular shape and orientation.^{53,55–57} All these factors affect the structure and dynamics of the supercooled liquid at its free surface,^{58–60} which, in turn, templates the properties of a vapor-deposited glass.⁶¹

One approach to independently study the role of each structural motif on the glass properties is to design homologous series of molecules where these variables can be tuned independently.^{8,50} In this study, we expand on our earlier approach⁸ of using high-throughput Suzuki cross coupling reactions to generate a library

of triarylbenzene molecules, homologous to tris(naphthyl)benzene (TNB), a well-characterized molecular glassformer.^{19,20,61,62} This approach allows us to systematically study the role of molecular weight, shape, intra-molecular degrees of freedom, and molecular level interactions on the glass transition temperature and fragility, as well as indices of refraction and expansion coefficients of both SCL and glass states, through differential scanning calorimetry (DSC) and *in situ* spectroscopic ellipsometry (SE) experiments, with a capability to measure cooling rate-dependent T_g .^{8,63} The combination of the facile synthesis and simple and broadly accessible experimental techniques provides a wealth of data that can be used for future exploration using predictive design approaches.

The T_g values of compounds designed in this study span a range of ~ 150 K, starting from just above room temperature up to 452 ± 2 K, which is comparable or higher than common glassy and thermoplastic polymers, such as polystyrene, polycarbonate, and polyurethanes, making these molecular glasses and their analogs of potential interest in various applications, such as resist materials,⁹ organic electronics,^{64,65} 3D patterning,⁶⁶ and other coatings, where ductility may not be critical, but high thermal stability and high T_g are desirable. Molecular glasses with the same T_g as polymers

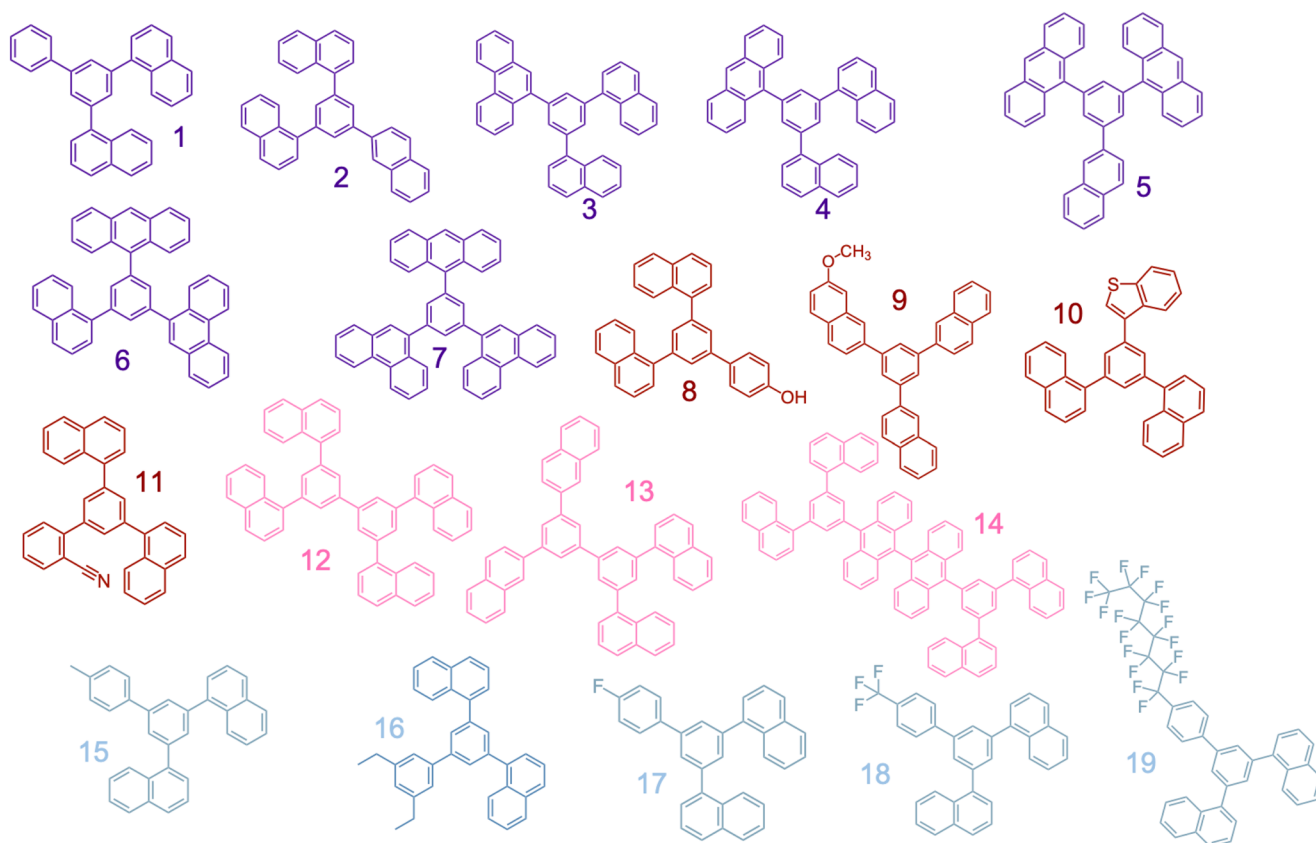


FIG. 1. Molecular structure of molecules 1–19. Structures are color-coded into several homologous series and organized as follows: the addition of aromatic substituents (purple), and the presence of heteroatoms other than fluorine (red), dimer compounds (pink), and compounds containing alkyl or fluorine alkyl chains (blue). Color-coding and compound numbers shown here are used throughout this article.

can be more processable for such applications as they do not have the high viscosity of entangled polymers, eliminating the need for additives and enabling preparation via physical vapor deposition or 3D printing.

II. METHODS

A. Synthesis of triarylbenzene molecules

The starting material, 1-bromo-3-chloro-5-iodobenzene, was synthesized by students enrolled in the Chemistry 245 class (Introduction to Organic Chemistry Laboratory) at the University of Pennsylvania. Procedures for this synthesis are detailed by Gilbert and Martin.⁵⁷ To synthesize compounds (1)–(19) shown in Fig. 1 (numbered for simplicity), palladium catalyzed Suzuki cross coupling reactions were used to couple aryl boronic acids with aryl halides to form biaryl linkages. The final products were characterized using nuclear magnetic resonance (NMR) measurements, ¹H NMR and ¹³C{¹H} NMR (Brüker AM-500 Fourier transform NMR spectrometer, 500 and 125 MHz). The synthesis of compounds 1, 2, 4, 5, and 12 was reported in our earlier publications.⁸ The details of the synthesis, purification, and NMR characterization of all other compounds are provided in the [supplementary material](#).

B. Differential scanning calorimetry

5–12 mg of each compound was mounted on T-zero Aluminum pans (TA Instruments) and sealed by using hermetic lids (TA Instruments). The pans were loaded into a Q2000 DSC instrument (TA Instruments). Two trials of heating (273–623 K) and cooling (623–273 K) ramps were performed on each compound using 10 K/min heating/cooling rates. Figure 2(a) shows an example of the normalized heat capacity for compound 4, measured upon cooling. As shown in Fig. 2(a), the glass transition ($T_{g,DSC}$) and the width of the glass transition ($\Delta T_{g,DSC}$) can be determined using the midpoint and the difference between the high onset (T_+) and the low onset (T_-), of the transition respectively. The heat capacity data of all newly synthesized compounds are shown in the [supplementary material](#). The heat capacity for compounds 1, 2, 5, and 12 was previously published.⁸ All $T_{g,DSC}$, $\Delta T_{g,DSC}$, and melting point (T_m , when melting was observed) values obtained from DSC measurements and those reported previously⁸ are listed in Table I.

C. Cooling rate-dependent T_g measurements using spectroscopic ellipsometry

Compounds 1–4, 8, 9, 17, and 18 were vapor-deposited as ~200 nm films in a custom vacuum chamber⁵⁰ (base pressure: 2×10^{-7} Torr) for further characterization. Each powdered compound was mounted into an aluminum oxide crucible (Lesker) and thermally evaporated onto RCA-cleaned silicon (100) substrates with 1 nm native oxide (Virginia Semiconductor, Inc.). The deposition rate was kept constant at 0.2 ± 0.03 nm/s. More details of the deposition procedure can be found in the [supplementary material](#) and in our earlier publications.^{8,50} As-deposited films were first annealed on a temperature-controlled stage (Linkam THMS600) to their corresponding $T_g + 20$ K for 10 min to erase their thermal history and produce liquid-quenched glass states upon cooling.

Dilatometry measurements were performed to characterize cooling rate-dependent $T_g(CR - T_g)$ values using *in situ* spectroscopic ellipsometry (SE, J.A. Woollam M-2000V). The spectroscopic wavelength range was chosen to be $550 \text{ nm} < \lambda < 1600 \text{ nm}$. Ellipsometric angles $\Psi(\lambda)$ and $\Delta(\lambda)$, which represent the ratio of *p*- and *s*-polarized reflection coefficients [$r_p/r_s = \tan(\Psi)e^{i\Delta}$], were measured as raw data. The film thickness and index of refraction were obtained by modeling the glass thin film as, a transparent Cauchy layer, where the real (*n*) and imaginary (*k*) parts of the index of refraction are defined as

$$n(\lambda) = A + \frac{B}{\lambda^2} \quad \text{and} \quad k = 0. \quad (1)$$

Here *A*, *B*, and film thickness (*h*) are fitting parameters. This model fits the data accurately in all compounds within the chosen

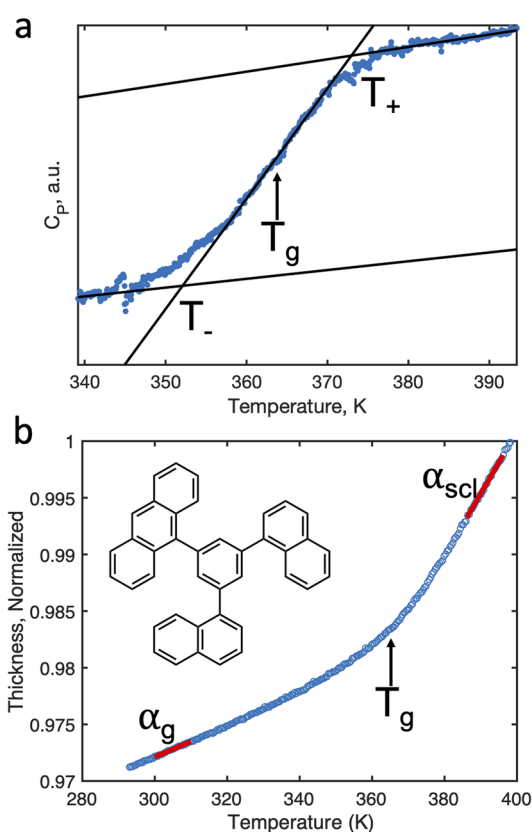


FIG. 2. (a) Heat capacity vs temperature, measured upon cooling at a rate of 10 K/min for compound 4. The three solid lines are linear fits to the glass, transition, and SCL lower onset temperature regions. The intersections are used to define T_+ and T_- , the high and lower temperature for transition, respectively. The midpoint of the transition is defined as $T_{g,DSC} = 362 \pm 4$. The width of the transition is defined as $\Delta T_{g,DSC} = T_+ - T_-$. Labeled are the locations of T_+ , T_- , and $T_{g,DSC}$. (b) Normalized thickness vs temperature, measured by spectroscopic ellipsometry upon cooling at a rate of 10 K/min for compound 4. The regions highlighted in red at low- and high-temperature regions of the curve were used to determine the expansion coefficients of the glass (α_{glass}) and the supercooled liquid (α_{SCL}), respectively. The arrow indicates the location of $T_{g,SE} = 364 \pm 1$ K. The structure of the compound is shown as the inset.

TABLE I. Numerical values of molecular weight (M_W) expressed in units of g/mol, melting point (T_m) obtained from DSC, glass transition temperature (T_g), the width of the transition (ΔT_g) obtained from both DSC and spectroscopic ellipsometry (SE) measurements, and dynamical fragility (m) obtained from SE. Horizontal lines separate various categories of compounds, as color-coded in Fig. 1. The values in bold are from external references.

Compound nos.	M_W (g/mol)	T_m (K)	$T_{g,DSC}$	$\Delta T_{g,DSC}$ (K)	$T_{g,SE}$ (K)	$\Delta T_{g,SE}$ (K)	m
1	406.53	417 ± 1⁸	331 ± 1⁸		333 ± 1	9	99 ± 21
2	456.59	464 ± 1⁸	343 ± 1⁸		343 ± 1	13	71 ± 29
3	506.65		363 ± 5	23	363 ± 2	21	62 ± 8
4	506.65	510 ± 2	362 ± 2	23	364 ± 1	17	72 ± 22
5	556.71	594 ± 3⁸	392 ± 1⁸				122⁸
6	556.71		382 ± 4	24			
7	606.77		389 ± 5	25			
8	422.53		344 ± 1	32	352 ± 1	17	99 ± 17
9	486.61	436 ± 1	333 ± 1	24	347 ± 1	15	81 ± 20
10	462.61		332 ± 2	26			
11	431.54		334 ± 2	20			
12	658.84	549 ± 2⁸	383 ± 1⁸				80⁸
13	658.84		378 ± 4	25			
14	1011.28		452 ± 2	25			
15	420.56		331 ± 2	20			
16	462.64	449 ± 2	310 ± 8	11			
17	424.52		322 ± 1	23	331 ± 1	11	116 ± 37
18	474.53		326 ± 2	17	328 ± 1	8	197 ± 27
19	824.58		307 ± 6	27	310 ± 2	14	

wavelength range (example shown in Fig. S39 of the [supplementary material](#)). During *in situ* measurements, SE was performed at a rate of ~1 data point every 2 s with zone-averaging. The temperature was recorded at the end of each data point.

For dilatometry experiments, nominal $T_{g,SE}$ was obtained upon cooling at $CR = 10$ K/min [example shown in Fig. 2(b)], consistent with the cooling rates used to obtain $T_{g,DSC}$. The samples were then heated to their corresponding $T_{g,SE} + 20$ K at a rate of 150 K/min and subsequently cooled at various cooling rates ranging from $CR = 150$ K/min down to $CR = 1$ K/min. Slower cooling rates ($CR \leq 60$ K/min) were generally the same as the value set by the instrument (Linkam THMS600 stage) to within 0.5 K/min, but faster rates were not always reached due to limitations in our cooling capacity. To eliminate errors, the actual cooling rates were calculated from the collected time-dependent temperature values (see Fig. S40 of the [supplementary material](#) for more details). In addition, the fast cooling rates were not always constant over the entire cooling range. If rates calculated over the full range were not the same as the cooling rates calculated within the window of $T_{g,SE} - 10$ K to $T_{g,SE} + 10$ K, then that data point was not used. This measure generally removed 1–4 cooling ramps from a typical dataset, so there remained at least five datasets at various cooling rates. To ensure that the films did not change their properties over the course of the experiment, either due to dewetting or degradation, an additional cooling ramp at the fastest rate was performed at the end of each cycle to compare with the data obtained during the first cooling cycle.

For each SE dataset, the thickness was normalized to the value of thickness at the maximum temperature of the $CR - T_g$ experiments. An additional correction was performed to obtain the actual temperature of the sample during the scan as opposed to the value recorded at the end by averaging each temperature with the previously recorded temperature. T_g was then determined for each cooling rate as the intersection of linear fits to the SCL and glassy regimes. An example of normalized thickness vs temperature for various cooling rates for compound **1** is shown in Fig. 3(a) after these corrections were applied. As shown in Fig. 3(a), the supercooled liquid (SCL) lines for all cooling rates overlap well, which validates this approach. We note that despite these measures to improve the accuracy of the data, the values of T_g at high cooling rates have larger errors due to the limited number of data points, which affects the accuracy of determining the fragility index, m . Future experiments can use flash DSC or dielectric spectroscopy experiments, which enable data over a much broader range of cooling rates and relaxation times.

The cooling rate at T_g is an indirect measure of the inverse of structural relaxation time, τ_α . A cooling rate of 10 K/min typically corresponds to a relaxation time of $\tau_\alpha \sim 100$ s ($CR \times \tau_\alpha \approx 1000$). As such, a plot of CR vs $1/T_g$ [Fig. 3(b)] can provide an indirect measure of τ_α vs $1/T$ [right axis in Fig. 3(b)].^{8,63,68,69} Given the limited range of CR 's available in this study, the data for various compounds can be fitted using an Arrhenius relationship [solid lines in Fig. 3(b)],

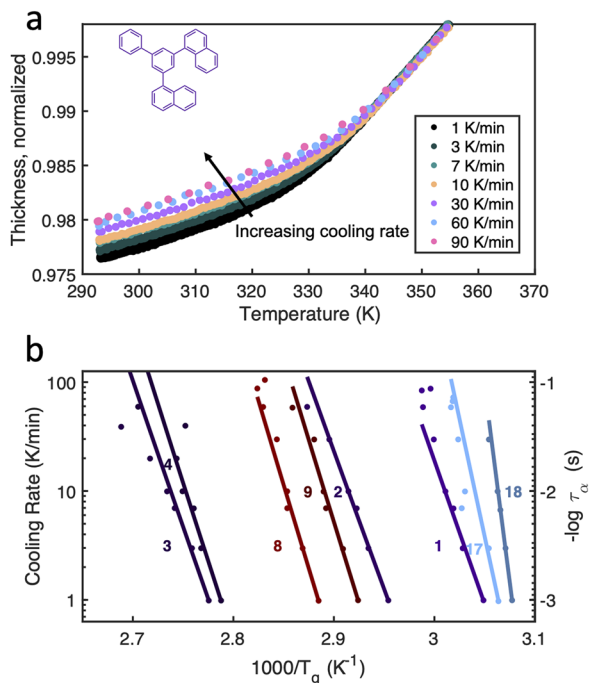


FIG. 3. (a) SE-based dilatometry measurements on compound 1 (structure shown in the inset). The curves show thickness vs temperature at various cooling rates, normalized to the thickness at 358 K. (b) Cooling rate (CR) vs $1000/T_g$ for compounds 1–4, 8–9, 17, and 18. The estimated τ_α values are shown on the right axis. The y axis is in log scales. Lines are Arrhenius fits to the data for each compound.

$$CR = CR_0 \exp\left(\frac{E_a}{k_B T}\right), \quad (2)$$

where CR_0 is a constant, k_B is the Boltzmann constant, and E_a is the apparent activation energy at T_g . The fragility index, m , is defined at T_g as⁴

$$\lim_{T \rightarrow T_g} m = \frac{d \log(\tau)}{d\left(\frac{T_g}{T}\right)} \approx \log e \times \frac{E_a}{k_B T_{g,SE}}. \quad (3)$$

The estimated values of m for various compounds are listed in Table I.

Spectroscopic ellipsometry provides a rich array of other material properties. The apparent expansion coefficients for the supercooled liquid (α_{SCL}) and glass (α_{Glass}) regions can be determined using the slope of the thickness change with temperature in the SCL and glass states, respectively ($\alpha = \frac{1}{h} \frac{dh}{dT}$), in regions highlighted in Fig. 2(b). These values were obtained by averaging the data over the same range at various slow cooling rates ($CR \leq 10$ K/min), where the data are more accurate, given the large number of collected data points and our improved ability to maintain a constant cooling rate. It is important to note that while this equation is accurate for the SCL regime, where the system is locally at equilibrium, the stresses produced due to the mismatch between the expansion coefficients of the glass film and the silicon substrate upon cooling can result in a discrepancy between the apparent values of α_{Glass} and its true values.⁷⁰ As such, the measured values are likely smaller than the true expansion coefficients of the bulk glass states.⁶³ Indices of refraction of the glass (n_{Glass}) and SCL (n_{SCL}) states were also determined from SE experiments using Eq. (1) at $T_{g,DSC} - 10$ K and $T_{g,DSC} + 10$ K, respectively. All values of n are reported at a wavelength of $\lambda = 632.8$ nm. The corresponding values at other wavelengths can be calculated using Eq. (1) and the A and B values obtained from the ellipsometry fitting for each compound at each temperature. These data are reported in Table II.

III. RESULTS AND DISCUSSION

A. Glass transition temperature and fragility

Figure 4(a) shows T_g vs molecular weight (M_W) for all compounds (values listed in Table I). We note that the molecular weight values here are expressed in units of g/mol, or molar mass, for

TABLE II. Calculated values of indices of refraction (n at $\lambda = 632.8$ nm) and expansion coefficients (α) for the supercooled liquid and glass states of various compounds. The typical error in determining n is $\delta n = 0.005$ based on the instrumental and reproducibility errors of SE experiments. The horizontal lines separate various categories of compounds, as color-coded in Fig. 1. The values in bold are from external references.

Compound nos.	n_{SCL}	n_{Glass}	$\alpha_{SCL} (10^{-4} K^{-1})$	$\alpha_{Glass} (10^{-4} K^{-1})$
1	1.706	1.712	5.81 ± 0.07	1.84 ± 0.04
2	1.722	1.728	5.60 ± 0.07	1.57 ± 0.02
3	1.726	1.730	5.45 ± 0.05	1.38 ± 0.01
4	1.730	1.735	5.63 ± 0.03	1.34 ± 0.04
5	1.756	1.760	4.02 ± 0.20^8	1.35 ± 0.03^8
8	1.712	1.715	5.76 ± 0.07	1.17 ± 0.09
9	1.724	1.728	5.42 ± 0.07	1.48 ± 0.04
12			5.30 ± 0.10^8	1.38 ± 0.02^8
17	1.694	1.697	5.5 ± 0.1	1.50 ± 0.04
18	1.656	1.661	6.0 ± 0.3	2.25 ± 0.07
19	1.545	1.551	7.46 ± 0.4	2.5 ± 0.09

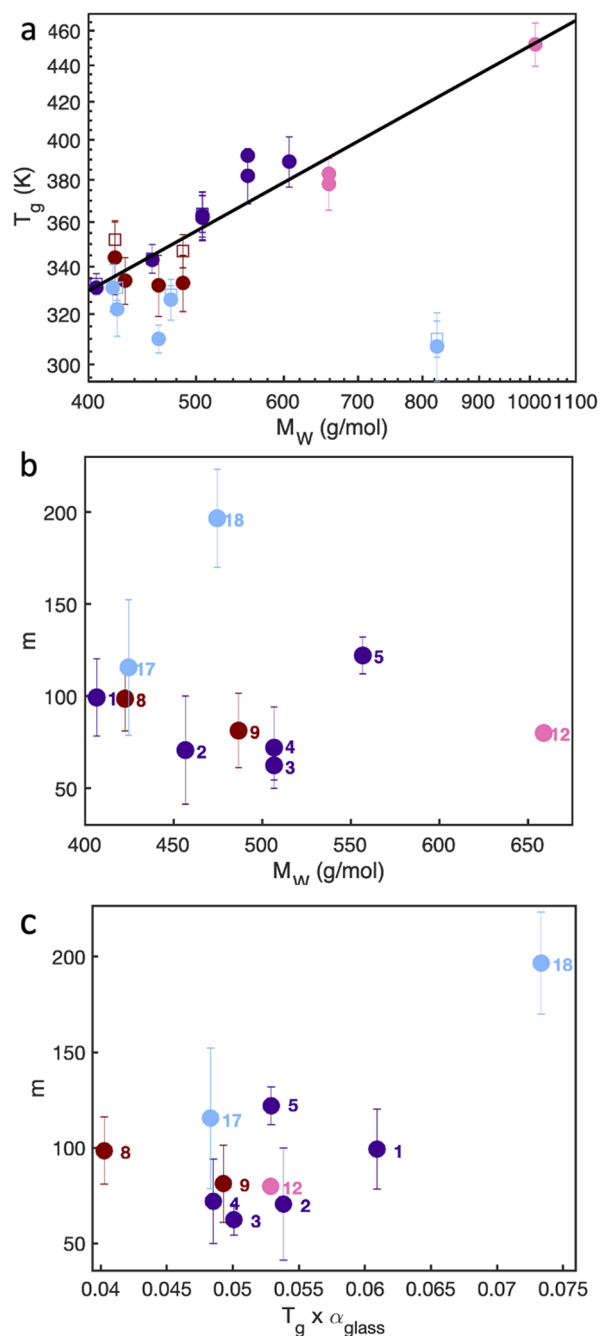


FIG. 4. (a) A log-log plot of $T_{g,DSC}$ (filled circles) and $T_{g,SE}$ (open squares) vs M_W for the library of compounds shown in Fig. 1. The black solid line represents a power-law fitting with an exponent of $\nu = 0.3 \pm 0.1$. The fit excludes T_g values for alkyl and fluoroalkyl containing compounds (15–20, blue data points). The vertical bars in this plot represent the width of the T_g transition (ΔT_g). Error bars based on repeated measurements (listed in Table I) are smaller than the symbol size and are not shown. (b) Dynamic fragility index (m) vs M_W for various compounds, obtained from $CR - T_g$ experiments. The values for compounds 5 and 12 are obtained from Ref. 8. (c) Fragility index (m) vs the product of $T_{g,DSC}$ and the expansion of the glassy line (α_{Glass}). The color coding based on categories of compounds shown in Fig. 1.

simplicity and ease of comparison with polymeric systems. The T_g values of these compounds span a range of ~ 150 K, starting from just above room temperature up to ~ 450 K. Within this range, a strong positive correlation is observed between T_g and M_W , with the exception of alkyl (compounds 16 and 15) or fluoroalkyl (compounds 17–19) containing compounds. Within the scatter of the data, the relationship between T_g and M_W follows a power-law dependence ($T_g \propto M^\nu$) with $\nu = 0.3 \pm 0.1$. These results are consistent with previous experimental and theoretical predictions of $0.3 < \nu < 0.5$.^{5,7,10,12–16}

Figure 5 plots these data along with an expansive set of data previously reported by Novikov and Rössler¹⁰ with T_g values ranging from 80 to 450 K and a power-law exponent of 0.51. While the T_g values in this study are generally higher than the average values at the same M_W and show a smaller power-law exponent, our data generally fall within the range of the scatter of this plot. Given that we study a homologous set of molecules, a stronger correlation is not surprising, as previous measurements have indicated that even higher exponents may be observed when strongly interacting substituents are systematically included.¹³

Despite the strong positive correlation of T_g with M_W , this correlation is not perfect. For example, when compounds 2, 10, and 16 with similar molecular weights are compared, their T_g values can differ by up to 30 K, which is slightly above the breadth of the glass transition within a single compound (typically 10–25 K, as seen in Table I). While these variations are still within the overall T_g scatter observed previously (Fig. 5), they can provide a window into understanding the role of structural details and inter-molecular interactions in glass transitions. For example, compound pairs 5/6 and 12/13 have slightly different T_g values despite having the same molecular weight. The low T_g in compounds 6 and 13 relative to their respective isomers may be the result of either decreased intra-molecular barriers of rotation of their substituents or increased

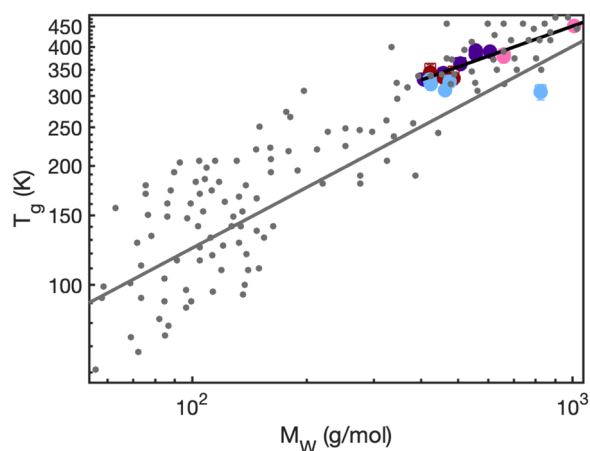


FIG. 5. T_g vs M_W data from this work (color-coded according to Fig. 1) and work from Novikov and Rössler¹⁰ (gray data points), showing that within the scatter, a power-law relationship is observed over a wide variety of organic glass-formers and wide range of T_g values (60–475 K). The black solid line is fit to the T_g values from this work ($\nu = 0.3 \pm 0.1$), and the gray solid line ($\nu = 0.51$) is the exponent fit extracted from Fig. 1 in Ref. 10 using WebPlotDigitizer.⁷¹

π - π stacking as a result of this flexibility. The observation that β substituents can lower T_g is consistent with those observed in tris(naphthyl)benzene isomers^{19,20} and their stable glasses.⁷² Future measurements of the entropy and enthalpy of these compounds and detailed studies of their structure and relaxation dynamics can better elucidate the origins of these effects.

Inter-molecular interactions and packing structure can also affect the details of the glass transition. The addition of a hydroxyl group in **8** increases its T_g compared to **15** and **1** with similar structures (Table I) and beyond compounds **2**, **9–11**, and **15–19**, all of which have higher molecular weights. The addition of the hydroxyl group appears to have stronger effects on T_g than nitrile (**11**) or thiophene (**10**). This is likely due to intramolecular hydrogen bonding, although investigation of further compounds can confirm this hypothesis. In contrast, the addition of ethyl substituents (**15** and **16**) or methoxy (**9**) groups results in a dramatic reduction in T_g . Similarly, both compounds **9** and **10** have lower T_g values than compound **2**, which is not immediately obvious. To understand the origins of these effects, a more focused structure/activity relation study will be necessary. Both intra- and inter-molecular interactions can play a role in the properties of these two compounds, as various isomers of both **9** and **10** may also have differing T_g values. The most notable effect is observed by the addition of alkyl and fluoro-alkyl groups (compounds **15–19**), where increasing the number of alkyl or fluorine atoms and thus M_W decreases T_g . More detailed discussions on these observations are provided in Sec. III D.

Figure 4(b) shows the dynamic fragility index (m) for a subset of the compounds in the library, for which $CR - T_g$ experiments were performed (data shown in Table I). There is no apparent systematic dependence of fragility on M_W or on structural motifs, with the exception of fluoroalkyl containing molecules (**17** and **18**, and potentially alkyl containing molecules^{27,28} for which we do not have collected SE data). This is in contrast to previous work, suggesting the existence of a measurable correlation between fragility and molecular weight or T_g .^{8,39,73,74} The data are also not fully consistent with the suggestion that the number of rotatable bonds in a compound can affect m .⁷⁵ For example, a clear difference between isomers of 3/4 or heteroatom substituted derivatives **8/17** is not observed here. A simple product of T_g and expansion coefficient as it has been previously suggested^{40,41} is not a great predictor of m either [Fig. 4(c)]. Some theories of dynamical relaxations in deeply supercooled liquids have indeed suggested that M_W is not a strong factor in determining m , and instead, one should expect a stronger correlation with thermodynamical quantities, such as entropy and enthalpy, cohesive energy, and density.^{15,17,76} Future measurements of heat capacity, enthalpy and entropy, dielectric relaxation, density, and pressure dependence of T_g can elucidate the role of these factors.

B. Index of refraction

Figure 6 shows indices of refraction of glass (n_{Glass}), calculated at $T_{g,SE} - 10$ K, and the supercooled liquid (n_{SCL}), calculated at $T_{g,SE} + 10$ K, respectively. Overall, there is a positive trend of increasing n with increasing molecular weight, with the exception of fluorinated compounds (**17–19**), which show a surprisingly strong negative trend. We note that while a similar behavior is likely in alkyl

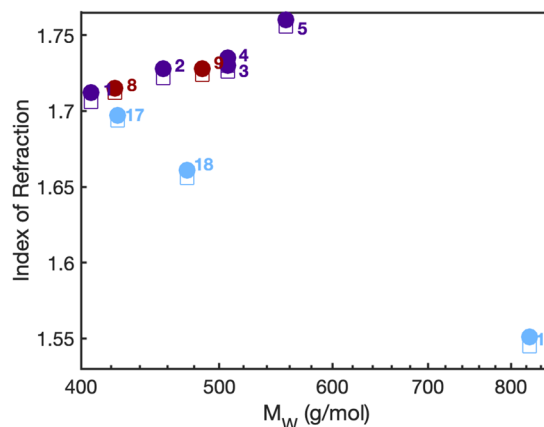


FIG. 6. Index of refraction, calculated at a wavelength of $\lambda = 632.8$ nm vs M_W for compounds **1**, **2–4**, **8**, **9**, and **17–19**. The filled and open symbols show n_{Glass} and n_{SCL} measured at $T_{g,DSC} - 10$ K and $T_{g,DSC} + 10$ K, respectively. Error bars are smaller than the symbol size. The x axis is shown in the log scale for clarity.

containing molecules, we do not have SE data for these molecules. The positive trend in n is consistent with previous empirical observations.⁷⁷ To better understand the origin of these trends, we note that the index of refraction in transparent materials depends on the polarizability of the molecule (μ) and density (ρ) through the Lorentz–Lorenz⁷⁸ equation,

$$\frac{n^2 - 1}{n^2 + 2} = \frac{\mu\rho}{3\varepsilon_0 M_W}, \quad (4)$$

where ε_0 is the permittivity of the free space. As such, the increasing value of n in compounds **1–5**, **8**, and **9** can be a sign of either increasing density with molecular weight or increasing polarizability in these conjugated π systems. To provide an estimate of the magnitude of these effects, we note that the difference in n between the SCLs to glass states of these molecules is 0.03–0.06 (Table II), while the corresponding density change between these two states is estimated to be 1% based on thickness variation through the transition (see Fig. 3, for example). As such, if the observed effects are purely due to the density variations, compounds **5** and **1** would have densities that differ by $\sim 10\%$ – 15% . This sets the upper bound for the density variations in these compounds. It is, however, important to note that increasing conjugation will likely also increase μ in these compounds. As such, the actual extent of density variations is expected to be much smaller than this upper bound.

This increase in density with M_W also means that T_g is correlated with ρ , as has been predicted in some theories of glass transition.^{15,17} Figure 7 shows the correlation between T_g and the Lorentz–Lorenz expression, indicating a strong correlation for these compounds. Interestingly, a weak but positive correlation is also observed for fluorinated compounds **17–19**. In these molecules, the Lorentz–Lorenz expression predicts a decrease in the density with increasing the length of perfluoroalkyl chains (increasing M_W), in particular for compound **19**. However, T_g of these compounds decreases rather modestly in comparison. The strong change in

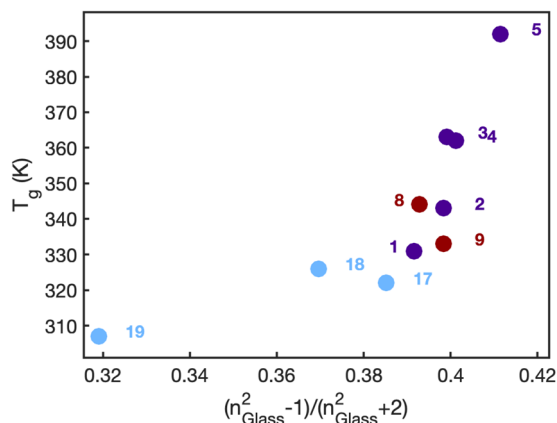


FIG. 7. The correlation plot between $T_{g,DSC}$ and $\frac{n_g^2 - 1}{n_g^2 + 2}$, where n_g is the index of refraction of the glass calculated at a wavelength of $\lambda = 632.8$ nm. From Eq. (4), the x axis is proportional to the product of density (ρ) and the polarizability (μ).

the slope of the correlation plot, compared to compounds that do not contain fluorine atoms, can be explained by the strong effect of fluorine on the polarizability, μ . Coarse-grained computer simulations have shown that in compound 19, the fluorinated alkyl chains lead to micro-phase separation of these domains from the bulky head groups,⁵³ which can explain the strong change in the density of the system due to packing frustrations, while the bulky domains contribute more strongly to the glass transition (more discussions in Sec. III D). Previous studies in ionic liquids have also indicated a trend of increasing micro-phase separation with increasing alkyl chain length, separating the polar and non-polar domains, consistent with observations in fluoroalkyl containing molecules.^{27,28}

C. Thermal expansion coefficients

Figures 8(a) and 8(b) show the apparent thermal expansion coefficients of the glass (α_{Glass}) and supercooled liquid (α_{SCL}) states, respectively. The trends of α_{Glass} and α_{SCL} appear to be in the opposite direction of trends in n , decreasing with M_W for most compounds except for the fluorinated series (17–19). A notable exception is the apparent α_{Glass} for compound 8, which is a hydroxyl containing molecule. In contrast to n , which continues to increase with M_W , the expansion coefficients appear to reach a plateau when $M_W \geq 500$ g/mol. To understand this behavior, we note that the thermal expansion coefficient is a measure of the anharmonicity of the inter-molecular interaction potential.⁴² Both increasing density and strong π -interactions can result in more harmonic local potentials. However, given the amorphous nature of these systems, non-zero anharmonicity is expected to persist even at high densities, explaining the plateau in values.

D. Alkyl and fluoroalkyl containing compounds

Compounds highlighted by blue in Fig. 1 (15–19) generally show an opposite property dependence to M_W compared to other

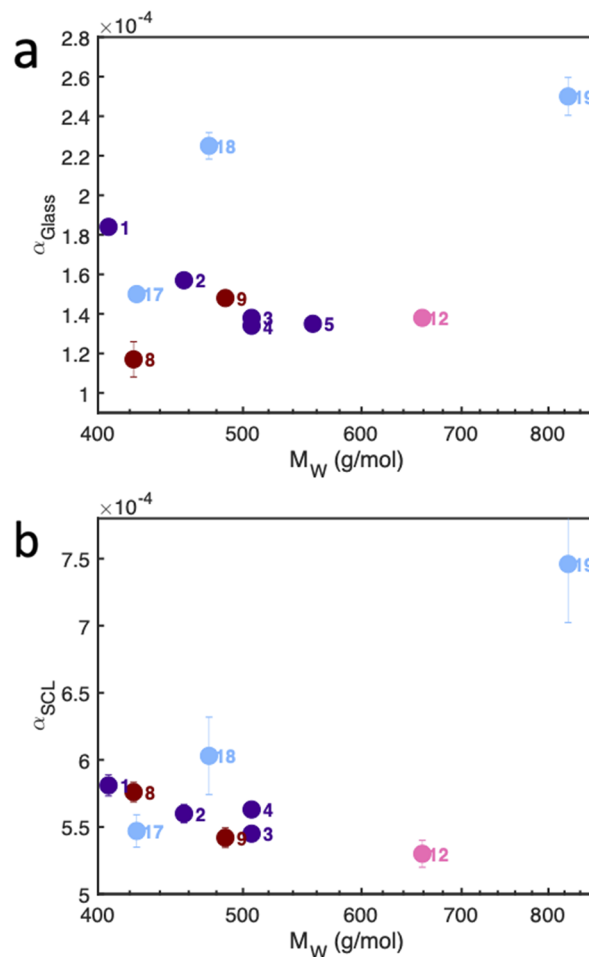


FIG. 8. (a) Thermal expansion coefficient of the glass (α_{Glass}) vs M_W for compounds 1–5, 4, 8, 9, 12, and 17–19. (b) Thermal expansion coefficient of the supercooled liquid (α_{SCL}) vs M_W for compounds 1–4, 8, 9, and 17–19. The x axis is shown on log scale for better clarity. The values for compounds 5 and 12 are obtained from Ref. 8.

compounds studied here. In particular, fluorinated and alkylated compounds generally show decreasing T_g [Fig. 4(a)], increasing fragility [Fig. 4(b)], decreasing n (Fig. 6), and increasing expansion coefficients (Fig. 8) upon increasing the fluoroalkyl chain length (and thus M_W). Fluorine atoms are strongly electronegative, which can lead to a lower dielectric constant and therefore lower polarizability, as well as decreased packing efficiency, which eventually leads to micro-phase separation when the fluoroalkyl chain size is increased.⁵³ The lower packing efficiency can explain the decreased density and increased anharmonicity (and thus increased expansion coefficients) and the increased fragility in these systems, all of which are expected to affect T_g . The low value of the dielectric constant of fluorine-containing materials (and thus polarizability) can also further affect the index of refraction and the Lorentz–Lorenz expression (Fig. 7).

These observations are consistent with the lower T_g values often observed in fluoropolymers compared to their non-fluorinated

counterparts. However, the addition of fluoroalkyl groups has also been observed to increase T_g in some systems,^{79,80} as the details of packing may depend on the structure of the molecule/polymer of interest. It is also worth noting that while we did not systematically explore the role of increased alkyl chain length on the packing in this study, long aliphatic chains can also disturb the packing, decrease T_g ,^{82–86} and increase fragility⁸⁶ by spreading the molecules further apart. Extremely long side chains may become sufficiently ordered as to result in micro-phase separation and crystallization. We have coarse-grained simulation data, indicating that a micro-phase separation as opposed to crystallization is likely in **19**,⁵³ which is consistent with the generation of packing frustration by fluoroalkyl or alkyl chains. Furthermore, compounds **15** and **16** also show surprisingly low T_g values, consistent with this explanation. As such, the origin of the behavior of fluoroalkyl containing molecules may, in fact, be independent of their fluorine content and more dependent on the presence of long chains that can disrupt packing, analogous to observations in ionic liquids.^{27,28}

Investigation of other non-polar molecules containing long alkyl chains or addition of multiple chains on the same molecule may help elucidate the origin of this behavior. It is not clear how the micro-phase separation affects the observed properties, given that it has been only produced in **19**. Future experiments can explore such effects by including fluoroalkyl groups of various lengths, making fluoro-containing dimers analogous to series **12–14**, or including fluorophenyl benzene substituents in the structure. Direct measurements of structure, density, and entropy/enthalpy of these compounds can help determine the role of density vs other factors in these observations.

IV. SUMMARY AND CONCLUSIONS

This study considered a library of similar organic glassformers to probe the influence of structural variations on the glass transition properties. This library of compounds spans a broad range of molecular weights and T_g values from room temperature to 450 K. The T_g index of refraction and expansion coefficients were observed to correlate with M_w , while fragility was relatively independent of M_w , spanning a range of 50–200. However, molecular level interactions and intra-molecular degrees of freedom were also seen to affect thermal properties for molecules with similar molecular weights. The synthesis technique used in this study enables systematic and detailed studies of such effects. The synthesis approach provided here can enable further studies of the effect of molecular structure on glass transition physics, beyond simple considerations of inter-molecular interactions that are often studied in computer simulations. Studies of the structure, relaxation dynamics, and entropy/enthalpy of these systems, as inter- and intra-molecular interactions are varied, can further illuminate structure/property relationships that can be used to compare with theoretical predictions.^{15,17} Across all properties, the presence of alkyl and fluoroalkyl motifs created strong deviations from otherwise observed properties, decreasing T_g with the increasing chain size and number of chains, increasing fragility, and increasing the expansion coefficients. Most of these effects can be attributed to the density and packing of the molecules, which are indirectly probed through the index of refraction. While more extensive studies of thermal and structural properties can provide a more detailed picture, the two

simple characterization techniques, calorimetry and spectroscopic ellipsometry, can be employed as high-throughput screening methods to quickly identify molecules of interest. The data generated here are added to a new database,⁸⁷ which is publicly available and will be expanded in the future by us and the research community to enable development of structure/property relationships in high molecular weight glassformers.

SUPPLEMENTARY MATERIAL

See the [supplementary material](#) for details of synthesis and characterization, details of DSC and ellipsometric measurements, and a correlation plot showing the comparison of T_g values of compounds in this study with those reported by Novikov and Rössler.¹⁰

ACKNOWLEDGMENTS

This research was primarily supported by the National Science Foundation NSF-DMREF (Grant No. DMR-1628407) and partially through the University of Pennsylvania Materials Research Science and Engineering Center (MRSEC) under Grant No. DMR-1720530. P.J.W. acknowledges funding from the NSF (Grant No. CHE-190250). The authors would like to thank undergraduate students in the Chemistry 245 laboratory course who synthesized 1-bromo-3-chloro-5-iodobenzene in class and Kim Mullane and Sharan Mehta for help in collecting the synthesized material.

AUTHOR DECLARATIONS

Conflict of Interest

The author have no conflicts to disclose.

Author Contributions

S.E.W., S.G., T.L., and A.Z. prepared glass samples of compounds that were synthesized and purified by H.Z., K.A., K.C., E. S.-R, G.H., F.G., A.Z., T.G.T., Y.W., and Y.P., who also performed NMR measurements. DSC experiments were performed by T.L., S.E.W., S.G., and Y.J. Ellipsometry experiments were performed by T.L. and S.E.W. Data analysis was performed by S.E.W. and A.Z. Data were added to database by S.G. and J.C. The manuscript was written by S.E.W., T.L., P.J.W., and Z.F. with the [supplementary material](#) written, in part, by K.C., Y.W., and H.Z. The project was designed and supervised by P.J.W. (synthesis) and Z.F. (sample preparation and characterization). Z.F. managed the project.

DATA AVAILABILITY

The details of synthesis and measured values of T_g , m , α , and n are reported at the Penn Glass Database.⁸⁷ All other data that support the findings of this study are available from the corresponding authors upon reasonable request.

REFERENCES

- ¹M. D. Ediger, C. A. Angell, and S. R. Nagel, "Supercooled liquids and glasses," *J. Phys. Chem.* **100**, 13200–13212 (1996).
- ²C. A. Angell, K. L. Ngai, G. B. McKenna, P. F. McMillan, and S. W. Martin, "Relaxation in glassforming liquids and amorphous solids," *J. Appl. Phys.* **88**, 3113 (2000).

- ³P. G. Debenedetti and F. H. Stillinger, "Supercooled liquids and the glass transition," *Nature* **410**, 259–267 (2001).
- ⁴C. A. Angell, "Formation of glasses from liquids and biopolymers," *Science* **267**, 1924–1935 (1995).
- ⁵C. A. Angell, J. M. Sare, and E. J. Sare, "Glass transition temperatures for simple molecular liquids and their binary solutions," *J. Phys. Chem.* **82**, 2622–2629 (1978).
- ⁶L.-M. Wang and R. Richert, "Glass transition dynamics and boiling temperatures of molecular liquids and their isomers," *J. Phys. Chem. B* **111**, 3201–3207 (2007).
- ⁷W. Ping, D. Paraska, R. Baker, P. Harrowell, and C. A. Angell, "Molecular engineering of the glass transition: Glass-forming ability across a homologous series of cyclic stilbenes," *J. Phys. Chem. B* **115**, 4696–4702 (2011).
- ⁸T. Liu, K. Cheng, E. Salami-Ranjbaran, F. Gao, E. C. Glor, M. Li, P. J. Walsh, and Z. Fakhraai, "Synthesis and high-throughput characterization of structural analogues of molecular glassformers: 1,3,5-trisubstituted benzenes," *Soft Matter* **11**, 7558–7566 (2015).
- ⁹J. Dai, S. W. Chang, A. Hamad, D. Yang, N. Felix, and C. K. Ober, "Molecular glass resists for high-resolution patterning," *Chem. Mater.* **18**, 3404–3411 (2006).
- ¹⁰V. N. Novikov and E. A. Rössler, "Similar dependence of glass transition temperature on molecular mass in molecular glasses and polymers," *AIP Conf. Proc.* **1599**, 130–133 (2014).
- ¹¹A. L. Agapov and A. P. Sokolov, "Does the molecular weight dependence of T_g correlate to M_e ?", *Macromolecules* **42**, 2877–2878 (2009).
- ¹²V. N. Novikov and E. A. Rössler, "Correlation between glass transition temperature and molecular mass in non-polymeric and polymer glass formers," *Polymer* **54**, 6987–6991 (2013).
- ¹³F. Krohn, C. Neuber, E. A. Rössler, and H.-W. Schmidt, "Organic glasses of high glass transition temperatures due to substitution with nitrile groups," *J. Phys. Chem. B* **123**, 10286 (2019).
- ¹⁴S. Mirigian and K. S. Schweizer, "Unified theory of activated relaxation in liquids over 14 decades in time," *J. Phys. Chem. Lett.* **4**, 3648–3653 (2013).
- ¹⁵S. Mirigian and K. S. Schweizer, "Elastically cooperative activated barrier hopping theory of relaxation in viscous fluids. II. Thermal liquids," *J. Chem. Phys.* **140**, 194507 (2014).
- ¹⁶S. Mirigian and K. S. Schweizer, "Elastically cooperative activated barrier hopping theory of relaxation in viscous fluids. I. General formulation and application to hard sphere fluids," *J. Chem. Phys.* **140**, 194506 (2014).
- ¹⁷R. W. Hall and P. G. Wolynes, "Intermolecular forces and the glass transition," *J. Phys. Chem. B* **112**, 301–312 (2008).
- ¹⁸K. Koperwas, K. Adrjanowicz, Z. Wojnarowska, A. Jedrzejowska, J. Knapik, and M. Paluch, "Glass-forming tendency of molecular liquids and the strength of the intermolecular attractions," *Sci. Rep.* **6**, 36934 (2016).
- ¹⁹P. A. Bonvallet, C. J. Breitzkreuz, Y. S. Kim, E. M. Todd, K. Traynor, C. G. Fry, M. D. Ediger, and R. J. McMahon, "Organic glass-forming materials: 1,3,5-tris(naphthyl)benzene derivatives," *J. Org. Chem.* **72**, 10051–10057 (2007).
- ²⁰C. M. Whitaker and R. J. McMahon, "Synthesis and characterization of organic materials with conveniently accessible supercooled liquid and glassy phases: Isomeric 1,3,5-tris(naphthyl)benzenes," *J. Phys. Chem.* **100**, 1081–1090 (1996).
- ²¹T. Komatsu, "Application of fragility concept to metallic glass formers," *J. Non-Cryst. Solids* **185**, 199–202 (1995).
- ²²P. K. Gupta and J. C. Mauro, "Composition dependence of glass transition temperature and fragility. I. A topological model incorporating temperature-dependent constraints," *J. Chem. Phys.* **130**, 094503 (2009).
- ²³S. Martiello, D. R. Cassar, E. Alcobaça, and T. Botari, "Machine learning unveils composition-property relationships in chalcogenide glasses," [arXiv:2106.07749](https://arxiv.org/abs/2106.07749) (2021).
- ²⁴Y. Xia, B. Yuan, O. Gulbiten, B. Aitken, and S. Sen, "Kinetic and calorimetric fragility of chalcogenide glass-forming liquids: Role of shear vs enthalpy relaxation," *J. Phys. Chem. B* **125**, 2754–2760 (2021).
- ²⁵J. C. Mauro and A. K. Varshneya, "Multiscale modeling of arsenic selenide glass," *J. Non-Cryst. Solids* **353**, 1226–1231 (2007).
- ²⁶W. Zhu, M. Lockhart, B. Aitken, and S. Sen, "Dynamical rigidity transition in the viscoelastic properties of chalcogenide glass-forming liquids," *J. Non-Cryst. Solids* **502**, 244–248 (2018).
- ²⁷T. Cosby, Z. Vicars, M. Heres, K. Tsunashima, and J. Sangoro, "Dynamic and structural evidence of mesoscopic aggregation in phosphonium ionic liquids," *J. Chem. Phys.* **148**, 193815 (2018).
- ²⁸T. Cosby, U. Kapoor, J. K. Shah, and J. Sangoro, "Mesoscale organization and dynamics in binary ionic liquid mixtures," *J. Phys. Chem. Lett.* **10**, 6274–6280 (2019).
- ²⁹W. Xu, E. I. Cooper, and C. A. Angell, "Ionic liquids: Ion mobilities, glass temperatures, and fragilities," *J. Phys. Chem. B* **107**, 6170–6178 (2003).
- ³⁰V. Meenakshisundaram, J.-H. Hung, and D. S. Simmons, "Design rules for glass formation from model molecules designed by a neural-network-biased genetic algorithm," *Soft Matter* **15**, 7795–7808 (2019).
- ³¹R. Böhmer, K. L. Ngai, C. A. Angell, and D. J. Plazek, "Nonexponential relaxations in strong and fragile glass formers," *J. Chem. Phys.* **99**, 4201 (1993).
- ³²J. L. Green, K. Ito, K. Xu, and C. A. Angell, "Fragility in liquids and polymers: New, simple quantifications and interpretations," *J. Phys. Chem. B* **103**, 3991–3996 (1999).
- ³³D. Huang and G. B. McKenna, "New insights into the fragility dilemma in liquids," *J. Chem. Phys.* **114**, 5621 (2001).
- ³⁴R. Richert, K. Duvvuri, and L.-T. Duong, "Dynamics of glass-forming liquids. VII. Dielectric relaxation of supercooled tris-naphthylbenzene, squalane, and decahydroisoquinoline," *J. Chem. Phys.* **118**, 1828 (2003).
- ³⁵G. Ruocco, F. Sciortino, F. Zamponi, C. De Michele, and T. Scopigno, "Landscapes and fragilities," *J. Chem. Phys.* **120**, 10666–10680 (2004).
- ³⁶C. Dalle-Ferrier, A. Kisliuk, L. Hong, G. Carini, G. Carini, G. D'Angelo, C. Alba-Simionesco, V. N. Novikov, and A. P. Sokolov, "Why many polymers are so fragile: A new perspective," *J. Chem. Phys.* **145**, 154901 (2016).
- ³⁷V. N. Novikov and A. P. Sokolov, "Poisson's ratio and the fragility of glass-forming liquids," *Nature* **431**, 961–963 (2004).
- ³⁸K. Kunal, C. G. Robertson, S. Pawlus, S. F. Hahn, and A. P. Sokolov, "Role of chemical structure in fragility of polymers: A qualitative picture," *Macromolecules* **41**, 7232–7238 (2008).
- ³⁹Q. Qin and G. B. McKenna, "Correlation between dynamic fragility and glass transition temperature for different classes of glass forming liquids," *J. Non-Cryst. Solids* **352**, 2977–2985 (2006).
- ⁴⁰J. Krausser, A. E. Lagogianni, K. Samwer, and A. Zaccone, "Disentangling interatomic repulsion and anharmonicity in the viscosity and fragility of glasses," *Phys. Rev. B* **95**, 104203 (2017).
- ⁴¹A. K. Gangopadhyay, C. E. Pueblo, R. Dai, M. L. Johnson, R. Ashcraft, D. Van Hoesen, M. Sellers, and K. F. Kelton, "Correlation of the fragility of metallic liquids with the high temperature structure, volume, and cohesive energy," *J. Chem. Phys.* **146**, 154506 (2017).
- ⁴²F. H. Stillinger and P. G. Debenedetti, "Distinguishing vibrational and structural equilibration contributions to thermal expansion," *J. Phys. Chem. B* **103**, 4052–4059 (1999).
- ⁴³J.-H. Hung, T. K. Patra, and D. S. Simmons, "Forecasting the experimental glass transition from short time relaxation data," *J. Non-Cryst. Solids* **544**, 120205 (2020).
- ⁴⁴S. Yin, Z. Shuai, and Y. Wang, "A quantitative structure–property relationship study of the glass transition temperature of OLED materials," *J. Chem. Inf. Comput. Sci.* **43**, 970–977 (2003).
- ⁴⁵G. Chen, Z. Shen, A. Iyer, U. F. Ghumman, S. Tang, J. Bi, W. Chen, and Y. Li, "Machine-learning-assisted de novo design of organic molecules and polymers: Opportunities and challenges," *Polymers* **12**, 163 (2020).
- ⁴⁶S. Takeda, T. Hama, H.-H. Hsu, T. Yamane, K. Masuda, V. A. Piunova, D. Zubarev, J. Pitera, D. P. Sanders, and D. Nakano, "AI-driven inverse design system for organic molecules," [arXiv:2001.09038](https://arxiv.org/abs/2001.09038) (2020).
- ⁴⁷Y. Zhang and X. Xu, "Machine learning glass transition temperature of polymers," *Heliyon* **6**, e05055 (2020).
- ⁴⁸S. F. Swallen, K. L. Kearns, M. K. Mapes, Y. S. Kim, R. J. McMahon, M. D. Ediger, T. Wu, L. Yu, and S. Satija, "Organic glasses with exceptional thermodynamic and kinetic stability," *Science* **315**, 353–357 (2007).
- ⁴⁹A. Sepúlveda, M. Tylnski, A. Guiseppi-Elie, R. Richert, and M. D. Ediger, "Role of fragility in the formation of highly stable organic glasses," *Phys. Rev. Lett.* **113**, 045901 (2014).

- ⁵⁰T. Liu, K. Cheng, E. Salami-Ranjbaran, F. Gao, C. Li, X. Tong, Y.-C. Lin, Y. Zhang, W. Zhang, L. Klinge, P. J. Walsh, and Z. Fakhraai, "The effect of chemical structure on the stability of physical vapor deposited glasses of 1,3,5-triarylbenzene," *J. Chem. Phys.* **143**, 084506 (2015).
- ⁵¹M. Tylinski, Y. Z. Chua, M. S. Beasley, C. Schick, and M. D. Ediger, "Vapor-deposited alcohol glasses reveal a wide range of kinetic stability," *J. Chem. Phys.* **145**, 174506 (2016).
- ⁵²A. Laventure, A. Gujral, O. Lebel, C. Pellerin, and M. D. Ediger, "Influence of hydrogen bonding on the kinetic stability of vapor-deposited glasses of triazine derivatives," *J. Phys. Chem. B* **121**, 2350 (2017).
- ⁵³A. R. Moore, G. Huang, S. Wolf, P. J. Walsh, Z. Fakhraai, and R. A. Riggleman, "Effects of microstructure formation on the stability of vapor-deposited glasses," *Proc. Natl. Acad. Sci. U. S. A.* **116**, 5937–5942 (2019).
- ⁵⁴Y. Chen, Z. Chen, M. Tylinski, M. D. Ediger, and L. Yu, "Effect of molecular size and hydrogen bonding on three surface-facilitated processes in molecular glasses: Surface diffusion, surface crystal growth, and formation of stable glasses by vapor deposition," *J. Chem. Phys.* **150**, 024502 (2019).
- ⁵⁵K. J. Dawson, L. Zhu, L. Yu, and M. D. Ediger, "Anisotropic structure and transformation kinetics of vapor-deposited indomethacin glasses," *J. Phys. Chem. B* **115**, 455–463 (2011).
- ⁵⁶S. S. Dalal, D. M. Walters, I. Lyubimov, J. J. de Pablo, and M. D. Ediger, "Tunable molecular orientation and elevated thermal stability of vapor-deposited organic semiconductors," *Proc. Natl. Acad. Sci. U. S. A.* **112**, 4227 (2015).
- ⁵⁷T. Liu, A. L. Exarhos, E. C. Alguire, F. Gao, E. Salami-ranjbaran, K. Cheng, T. Jia, J. E. Subotnik, P. J. Walsh, J. M. Kikkawa, and Z. Fakhraai, "Birefringent stable glass with predominantly isotropic molecular orientation," *Phys. Rev. Lett.* **119**, 095502 (2017).
- ⁵⁸Y. Chen, M. Zhu, A. Laventure, O. Lebel, M. D. Ediger, and L. Yu, "Influence of hydrogen bonding on the surface diffusion of molecular glasses: Comparison of three triazines influence of hydrogen bonding on the surface diffusion of molecular glasses: Comparison of three triazines," *J. Phys. Chem. B* **121**, 7221–7227 (2017).
- ⁵⁹Y. Chen, W. Zhang, and L. Yu, "Hydrogen bonding slows down surface diffusion of molecular glasses," *J. Phys. Chem. B* **120**, 8007–8015 (2016).
- ⁶⁰S. Samanta, G. Huang, G. Gao, Y. Zhang, A. Zhang, S. Wolf, C. N. Woods, Y. Jin, P. J. Walsh, and Z. Fakhraai, "Exploring the importance of surface diffusion in stability of vapor-deposited organic glasses," *J. Phys. Chem. B* **123**, 4108–4117 (2019).
- ⁶¹J. H. Magill and D. J. Plazek, "Physical properties of aromatic hydrocarbons. II. Solidification behavior of 1,3,5-tri- α -naphthylbenzene," *J. Chem. Phys.* **46**, 3757 (1967).
- ⁶²I. Tsukushi, O. Yamamuro, T. Ohta, T. Matsuo, H. Nakano, and Y. Shirota, *J. Phys.: Condens. Matter* **8**, 245–255 (1996).
- ⁶³E. C. Glor and Z. Fakhraai, "Facilitation of interfacial dynamics in entangled polymer films," *J. Chem. Phys.* **141**, 194505 (2014).
- ⁶⁴S.-J. Zou, Y. Shen, F.-M. Xie, J.-D. Chen, Y.-Q. Li, and J.-X. Tang, "Recent advances in organic light-emitting diodes: Toward smart lighting and displays," *Mater. Chem. Front.* **4**, 788–820 (2020).
- ⁶⁵G. J. Hedley, A. Ruseckas, and I. D. W. Samuel, "Light harvesting for organic photovoltaics," *Chem. Rev.* **117**, 796–837 (2017).
- ⁶⁶D. Pires, J. L. Hedrick, A. De Silva, J. Frommer, B. Gotsmann, H. Wolf, M. Despont, U. Duerig, and A. W. Knoll, "Nanoscale three-dimensional patterning of molecular resists by scanning probes," *Science* **328**, 732–736 (2010).
- ⁶⁷J. Gilbert and S. Martin, *Experimental Organic Chemistry*, 4th ed. (Thomson Brooks/Cole, Belmont, CA, 2006), p. 708.
- ⁶⁸Y. Zhang, E. C. Glor, M. Li, T. Liu, K. Wahid, W. Zhang, R. A. Riggleman, and Z. Fakhraai, "Long-range correlated dynamics in ultra-thin molecular glass films," *J. Chem. Phys.* **145**, 114502 (2016).
- ⁶⁹T. Lan and J. M. Torkelson, "Fragility-confinement effects: Apparent universality as a function of scaled thickness in films of freely deposited, linear polymer and its absence in densely grafted brushes," *Macromolecules* **49**, 1331–1343 (2016).
- ⁷⁰J. E. Pye and C. B. Roth, "Physical aging of polymer films quenched and measured free-standing via ellipsometry: Controlling stress imparted by thermal expansion mismatch between film and support," *Macromolecules* **46**, 9455–9463 (2013).
- ⁷¹A. Rohatgi, Webplotdigitizer, copyright 2010–2021, <https://apps.automeris.io/wpd/>.
- ⁷²K. Dawson, L. Zhu, L. A. Kopff, R. J. McMahon, L. Yu, and M. D. Ediger, "Highly stable vapor-deposited glasses of four tris-naphthylbenzene isomers," *J. Phys. Chem. Lett.* **2**, 2683–2687 (2011).
- ⁷³A. Döb, M. Paluch, H. Sillescu, and G. Hinze, "From strong to fragile glass formers: Secondary relaxation in polyalcohols," *Phys. Rev. Lett.* **88**, 095701 (2002).
- ⁷⁴D. Heczko, K. Jurkiewicz, M. Tarnacka, J. Grelska, R. Wrzalik, K. Kamiński, M. Paluch, and E. Kamińska, "The impact of chemical structure on the formation of the medium-range order and dynamical properties of selected antifungal APIs," *Phys. Chem. Chem. Phys.* **22**, 28202–28212 (2020).
- ⁷⁵K. Kawakami, "Ultraslow cooling for the stabilization of pharmaceutical glasses," *J. Phys. Chem. B* **123**, 4996–5003 (2019).
- ⁷⁶L.-M. Martinez and C. A. Angell, "A thermodynamic connection to the fragility of glass-forming liquids," *Nature* **410**, 663–667 (2001).
- ⁷⁷R. H. Higgins, "A simple correlation of molecular weights and refractive indices," *J. Elisha Mitchell Sci. Soc.* **110**, 39–45 (1994).
- ⁷⁸C. J. F. Böttcher and P. Bordewijk, *Theory of Electric Polarization* (Elsevier Science Limited, 1978), Vol. 2.
- ⁷⁹D. W. Brown and L. A. Wall, "Glass transition temperatures of several fluorine-containing polymers," *J. Polym. Sci., Part A-2* **7**, 601–608 (1969).
- ⁸⁰M. Rowe, G. H. Teo, J. Horne, O. Al-Khayat, C. Neto, and S. C. Thickett, "High glass transition temperature fluoropolymers for hydrophobic surface coatings via RAFT copolymerization," *Aust. J. Chem.* **69**, 725–734 (2016).
- ⁸¹C. Fetsch and R. Luxenhofer, "Thermal properties of aliphatic polypeptides," *Polymers* **5**, 112–127 (2013).
- ⁸²D. J. Allen and H. Ishida, "Physical and mechanical properties of flexible polybenzoxazine resins: Effect of aliphatic diamine chain length," *J. Appl. Polym. Sci.* **101**, 2798–2809 (2006).
- ⁸³M. Soccio, N. Lotti, L. Finelli, M. Gazzano, and A. Munari, "Aliphatic poly(propylene dicarboxylate)s: Effect of chain length on thermal properties and crystallization kinetics," *Polymer* **48**, 3125–3136 (2007).
- ⁸⁴K. Kempe, E. F.-J. Rettler, R. M. Paulus, A. Kuse, R. Hoogenboom, and U. S. Schubert, "A systematic investigation of the effect of side chain branching on the glass transition temperature and mechanical properties of aliphatic (co-)poly(2-oxazoline)s," *Polymer* **54**, 2036–2042 (2013).
- ⁸⁵H. A. Schneider, "Polymer class specificity of the glass temperature," *Polymer* **46**, 2230–2237 (2005).
- ⁸⁶N. Soszka, B. Hachula, M. Tarnacka, E. Ozimina-Kamińska, J. Grelska, K. Jurkiewicz, M. Geppert-Rybczynska, R. Wrzalik, K. A. Grzybowski, S. Pawlus *et al.*, "The impact of the length of alkyl chain on the behavior of benzyl alcohol homologous. The interplay between dispersive and hydrogen bond interactions," *Phys. Chem. Chem. Phys.* **23**, 23796 (2021).
- ⁸⁷Penn glass database, <https://glass.apps.sas.upenn.edu>.